Int. J. Electrochem. Sci., 10 **(2015)** 725 - 736

International Journal of
ELECTROCHEMICAL
SCIENCE
www.electrochemsci.org

Electron-Transfer Kinetics of V(IV)/V(V) and V(II)/V(III) Couples for Different State of Charge

Fuyu Chen[1], *Hui Chen*[2], *Qing Sun*[1], *Jianguo Liu*[2], *Chuanwei Yan*[2], *Qingyu Liu*[1,*]

[1] College of Engineering, Shenyang Agricultural University, Shenyang 110866, China
[2] Laboratory for Corrosion and Protection, Institute of Metal Research, Chinese Academy of Sciences, Shenyang 110016, China
[*]E-mail: chenfuyu2005@163.com

Received: 13 October 2014 / *Accepted:* 19 November 2014 / *Published:* 2 December 2014

The electrochemical behavior of the V(Ⅳ)/V(Ⅴ) and V(Ⅱ)/V(Ⅲ) redox couples has been studied at a graphite electrode by cyclic voltammetry in sulfuric acid solutions. The diffusion coefficient (D) and the rate constant (k) of V(Ⅳ)/V(Ⅴ) and V(Ⅱ)/V(Ⅲ) redox couples for varying state of charge (SOC) can be calculated by cyclic voltammetry. The values of D_a(diffusion coefficient of anode) and k_a(the rate constant of anode) are increased for V(Ⅳ)/V(Ⅴ) couple while decreased for V(Ⅱ)/V(Ⅲ) couple with increasing of SOC. Electrochemical impedance spectroscopy (EIS) is employed to study mechanism of the two couples in sulfuric acid medium. Characteristic EIS plots with the capacitive semicircle in high frequency and the Warburg tail in low frequency are observed for the two couples, implying that both the electrochemical and diffusion process play important roles in V(Ⅳ)/V(Ⅴ) and V(Ⅱ)/V(Ⅲ) couples, the two electrode processes are controlled by both electron-transfer and mass-transfer.

Keywords: V(Ⅳ)/V(Ⅴ) couple; V(Ⅱ)/V(Ⅲ) couple; Electron-Transfer Kinetics; State of Charge

1. INTRODUCTION

Redox flow batteries (RFBs) are electrochemical energy storage devices that utilize the oxidation and reduction of soluble redox couples for charging and discharging. RFBs have several advantages [1-6] over some of the established conventional secondary batteries: long cycle life and relatively easily maintained; high battery efficiency; environmental friendly; deeply discharged without harm to the battery. So the RFB is thought to be ranked as the most promising one for the application of large scale energy storage among the electrochemical storage systems [7-8]. They are

appropriate for load leveling, uninterruptible power supply and distributed renewable power plants such as solar power plants and wind power plants.

Since the RFB concept was first proposed by Thaller [9] in 1974, several types of redox flow batteries have been developed [10-11]. For example, all-vanadium redox flow battery (VRB) system, which received considerable attention during the last years [12-19], employed two redox couples of V(Ⅳ)/V(Ⅴ) and V(Ⅱ)/V(Ⅲ) as the positive and the negative electrode active materials, respectively. The positive and the negative electrolyte which containing V(Ⅳ)/V(Ⅴ) and V(Ⅱ)/V(Ⅲ) active materials are stored in each electrolyte tanks and flowed through the electrode compartment by pumps. The capacity of the system is determined by the volume of the electrolyte tanks, while the system power is determined by the size of the stacks and the active electrode surface area. In contrast to usual secondary batteries which using solid active materials, VRB has a long cycle life and relatively large capacitance.

Despite these advantages, the vanadium redox flow battery has not been widely exploited to date. One disadvantage of the system developed to date is the imbalance in electron-transfer rate of V(Ⅳ)/V(Ⅴ) and V(Ⅱ)/V(Ⅲ) couples, which may result in charge and discharge imbalances and hydrogen [20] and oxygen evolution [21] in electrode compartments. Oxygen evolving reaction at positive electrode surface may cause corrosion of electrode [21]. Gas evolving reactions are consuming a portion of the current applied to the cell, reducing active surface area for reaction, which speed up charge and discharge imbalances and finally lead to declining of coulomb efficiency, energy efficiency and the capacity after repetitious systemic circulation of the battery. Therefore, it is important to study the electron-transfer kinetics of V(Ⅳ)/V(Ⅴ) and V(Ⅱ)/V(Ⅲ) couples during different state of charge (SOC) to improve energy efficiency and reduce capacity losses of VRB.

In this paper, electron-transfer kinetics of the two couples for different state of charge (SOC) was studied by cyclic voltammetry and electrochemical impedance spectroscopy (EIS). The variation of diffusion coefficient (D) and the rate constant (k) of them were presented in details and a full account of data analysis was showed by cyclic voltammetry, and then EIS plots studied mechanism of reactions. These experiments aimed to provide a preliminary indication of the relative performance of system.

2. EXPERIMENTAL

$VOSO_4 \cdot nH_2O$ (analytical reagent, n = 3.06 according to gravimetric analysis) of various concentrations were dissolved in 2M H_2SO_4. V(Ⅴ), V(Ⅲ) and V(Ⅱ) solutions were obtained by fully charging of V(Ⅳ) solution to V(Ⅴ) in the positive half-cell and fully discharging of V(Ⅳ) solution to V(Ⅲ) and V(Ⅱ) in the negative half-cell of a vanadium redox cell. All solutions were deaerated by bubbling with nitrogen prior to the experiments. A 50% SOC was corresponded to 50:50 mixture of V(Ⅳ) and V(Ⅴ) positive half-cell of a vanadium redox cell and the same as V(Ⅲ) and V(Ⅱ) in negative electrolyte. The different SOC of positive electrolyte was prepared by mixing definite volumes of V(Ⅳ) solution (0 % SOC) with V(Ⅴ) solution (100 % SOC). The different SOC of negative

electrolyte was prepared by mixing definite volumes of V(III) solution (0 % SOC) with V(II) solution (100 % SOC).

The electrochemical behavior of the V(IV)/V(V) and V(II)/V(III) couples were studied at a graphite electrode with a surface area of 0.07 cm^2 (spectroscopically pure). The electrode was polished with 1200 CCR/R and 2000 CCR/R silicon carbide polishing paper, followed successively by 5min ultrasonic cleaning and then rinsed thoroughly with distilled water. A saturated calomel electrode (SCE) electrode was used as a reference electrode and large-area (approximately 2 cm^2) platinum plate was used as the auxiliary electrode.

The electrochemical measurements were performed using a Princeton Applied Research (PAR) EG&G potentiostat model 273 and EG&G5210 lock-in amplifier with M398 testing software. All electrochemical measurements were conducted using a conventional three-electrode electrochemical cell with graphite as working electrode, a platinum plate as auxiliary electrode and a saturated calomel electrode (SCE) as reference. The scan rate of cyclic voltammetry was 50~ 250 $mV \cdot s^{-1}$. The signal amplitude of EIS was 5 mV and the frequency ranged between 1.0E-2 Hz and 1.0E-5 Hz. All the electrochemical measurements were conducted at room temperature.

3. RESULTS AND DISCUSSION

3.1. Reproducibility of electrode surface preparation

Sum et al.[13] previously reported that the preparation procedure for the electrode surface had a critical effect on the electrode kinetics of the vanadium redox couples at a glassy–carbon electrode. The first objective, therefore, was to examine the reproducibility of the surface preparation procedure on the behavior of the graphite electrode. Fig. 1(a) and (b) shows four positive and negative cyclic voltammograms that were obtained after successively repolishing the graphite electrode surface using the procedure described above, respectively. The curves in Fig. 1 showed that the reproducibility and stability obtained on the graphite electrode surface is well.

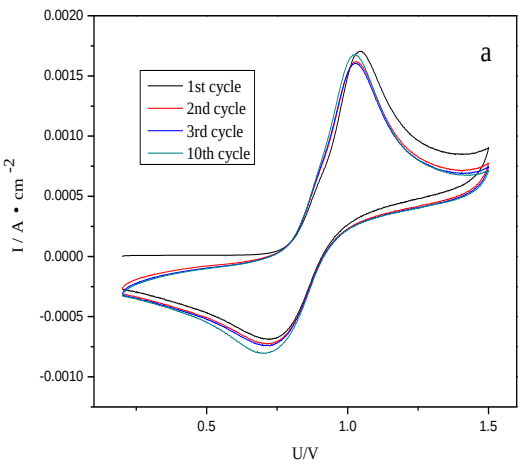

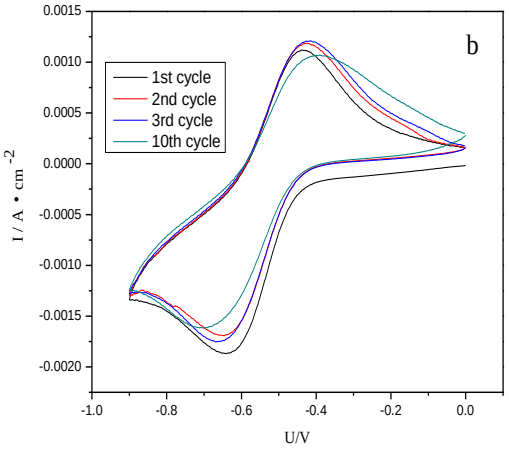

Figure 1. Cyclic voltammograms for graphite electrode in (a) 0.2 M V(Ⅳ)/2M H_2SO_4; (b) 0.2 M V(Ⅲ)/2M H_2SO_4 solution, sweep rate: 50 mV s^{-1}

Apart from the tenth cycle in negative voltammograms, only a slight variation can be observed among the remaining voltammograms. This confirms that the graphite electrode is suitable working electrode for studying the electrochemical behavior of the V(Ⅳ)/V(Ⅴ) and V(Ⅱ)/V(Ⅲ) couples.

3.2. Cyclic voltammetry of V(Ⅳ)/V(Ⅴ) and V(Ⅱ)/V(Ⅲ) couples

A series of cyclic voltammograms corresponding to the V(Ⅳ)/V(Ⅴ) and V(Ⅱ)/V(Ⅲ) couples at the graphite electrode at various sweep rates in 0.18 M V(Ⅴ) 90 % SOC positive and 0.36 M V(Ⅲ) 10 % SOC negative vanadium redox cell solution are presented in Fig. 2 and Fig. 3. As the minimum peak separation of positive and negative are 292 mV and 380 mV, respectively, the V(Ⅴ) + $e^- \Leftrightarrow$ V(Ⅳ) and V(Ⅲ) + $e^- \Leftrightarrow$ V(Ⅱ) reactions are irreversible at the graphite electrode. For an irreversible reaction, the peak current, i_p, is given by [22]:

$$i_p = 0.4958n^{3/2}F^{3/2}A\alpha^{1/2}\,CD^{1/2}\nu^{1/2}(RT)^{-1/2} \qquad (1)$$

Where i_p is the peak current (Amperes), A is the electrode area (cm^2), C is the bulk concentration ($mol \cdot L^{-1}$), ν is the potential sweep rate ($mV \cdot s^{-1}$), D is the diffusion coefficient of the particles ($cm^2 \cdot s^{-1}$), α is the transfer coefficient and n is the number of electrons involved in the rate-determining step.

A plot of i_p vs. $\nu^{1/2}$ should therefore give a straight line with slope proportional to D. For a totally irreversible process, the peak potential, E_p, is a function of scan rate, the difference between E_p and the formal potential, E_0, being related to the heterogeneous rate constant, k.

The peak current may also be expressed as [22]:

$$i_p = 0.227nFACk \exp[-\frac{\alpha nF}{RT}(E_p - E_0)] \qquad (2)$$

A plot of ln (i_p) vs. (E_p- E_0), determined at different scan rates, should thus have a slope of –(αnF/RT) and an intercept proportional to k.

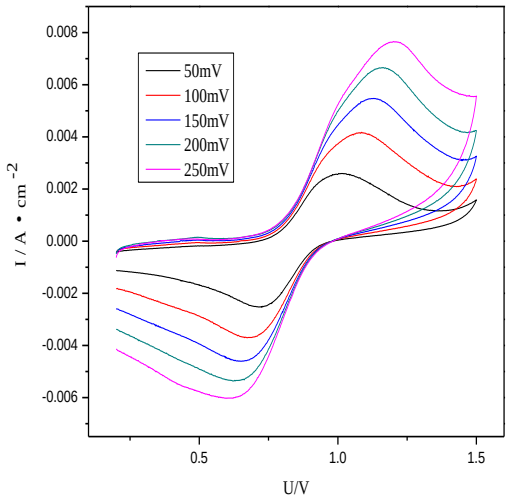

Figure 2. Cyclic voltammograms for V(Ⅳ)/V(Ⅴ) couple for 90% SOC

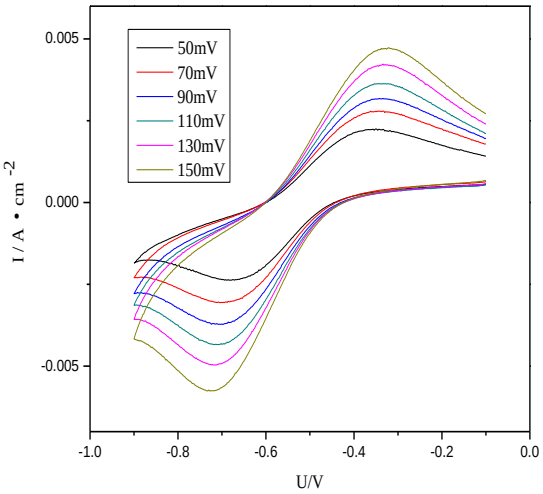

Figure 3. Cyclic voltammograms for V(Ⅱ)/V(Ⅲ) couple for 10% SOC

Plots of positive ln (i_p) vs. (E_p- E_0) and peak current, i_p, vs. $v^{1/2}$ for the cyclic voltammograms of Fig. 2 are given in Fig. 4 and Fig. 5. Assuming a value of k_a equal to 2.98×10^{-3} cm·s^{-1} and k_c to 1.46×10^{-4} cm·s^{-1}. The values of the anodic and cathodic diffusion coefficient calculated from the slope of straight line are 6.35×10^{-5} cm^2·s^{-1} and 2.14×10^{-7} cm^2·s^{-1}, respectively. Similar plots are performed from cyclic voltammograms obtained for various SOC of positive and negative electrolyte, respectively. The influence of SOC for positive and negative electrolyte on the parameters k and D is summarized in Table 1 and Table 2. The data suggests that the electron transfer of V(Ⅱ)/V(Ⅲ) is much slower than that of V(Ⅳ)/V(Ⅴ) couple at graphite electrode.

Systemic analyses of parameters k and D for different SOC is showed in Fig. 6, which indicate that the anodic rate constant (k_a) and the diffusion coefficient (D_a) of V(Ⅳ)/V(Ⅴ) couple improve with

SOC increasing, corresponding to the reduction of cathodic rate constant (k_c) and the diffusion coefficient (D_c).

According to Nernst equation: $E = E_0 + \frac{RT}{nF}\ln\frac{C_O}{C_R}$, C_0 and C_R are the bulk concentration of oxidation and reduction. At a normal temperature, the value of C_0/C_R is increased as the SOC improving for V(Ⅳ)/V(Ⅴ) couple, which enhances the values of $\frac{RT}{nF}\ln\frac{C_O}{C_R}$, therefore, the electrode potential (E) that acts on V(Ⅳ) + e →V(Ⅴ) reaction is improved significantly. According to the influence of electrode potential to activation energy of electrochemical process, the growth of electrode potential reduces anodic activation energy so that the electron transfer rate of oxidation reaction is speeded up, which corresponding to large k_a. Also, the growth of electrode potential improves cathodic activation energy, the process of cathode reaction is slow down. Thus cathodic rate constant (k_c) decreases as the rising of SOC, as presented in Fig. 6(a).

The variation of diffusion coefficients (D) for V(Ⅳ) + e^- ⇔ V(Ⅴ) reaction are showed in Fig. 6(a) based on eqn.(1). As the SOC improving for V(Ⅳ)/V(Ⅴ) couple, the electrode potential (E) that acts on V(Ⅳ) + e →V(Ⅴ) reaction is improved and reduction concentration of V(Ⅳ) is reduced. The growth of electrode potential improves anodic peak current (i_p) while reduces concentration of V(Ⅳ) with rising of SOC. Assuming a value of αn equal to 0.5, the value of anodic diffusion coefficient (D_a) calculated from the slope of straight line grows as the rising of SOC. The value of D_c reverses variation of D_a.

Above-mentioned are kinetics parameters for V(Ⅳ)/V(Ⅴ) couple, the variation of rate constant (k) and diffusion coefficient (D) of V(Ⅱ)/V(Ⅲ) couple comply with the regulation of V(Ⅳ)/V(Ⅴ) couple. Data in Fig. 6(b) suggest that cathodic rate constant (k_c) and diffusion coefficient (D_c) go up along with the rising of SOC.

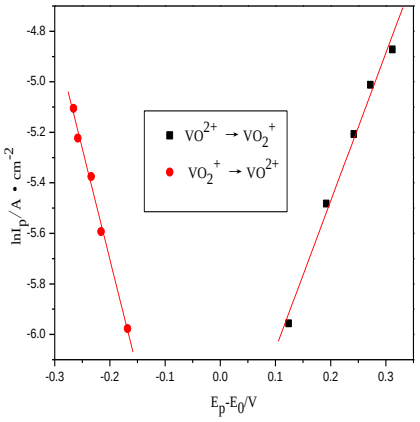

Figure 4. Plots of $\ln i_p$ vs.(E_P-E_0) for V(Ⅳ)/V(Ⅴ) couple for 90% SOC

The theory employed in this paper for the mathematical treatment of the results assumes that the electrode surface is smooth. The use of the 2000 CCR/R sandpaper would give rise to a certain degree of electrode roughness, which could cause problems in the application of the theory to the

treatment of results in this study. This reason would help to explain the variational consistency of results as presented in Fig. 6 and Fig. 7. Data in Fig. 7 validate the results in Fig. 6 that reaction rate of mixing valence state of vanadium ions is faster than that of one single valence state in electrolyte.

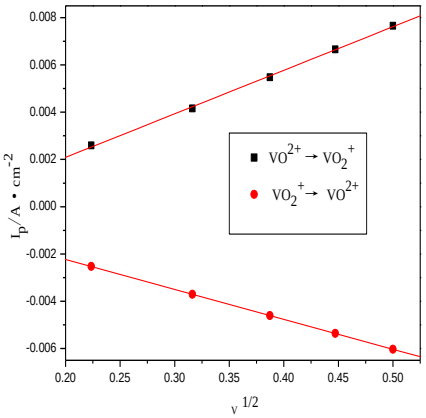

Figure 5. Plots of i_p vs. $\nu^{1/2}$ for V(Ⅳ)/V(Ⅴ) couple for 90% SOC

Table 1. Diffusion coefficient and rate constants of V(Ⅳ)/V(Ⅴ) couple for different SOC

SOC/%	k_a/cm·s^{-1}	k_c/cm·s^{-1}	D_a/cm^2·s^{-1}	D_c/cm^2·s^{-1}
90 (V(Ⅳ)=0.02 M)	2.98×10^{-3}	1.46×10^{-4}	6.35×10^{-5}	2.14×10^{-7}
70 (V(Ⅳ)=0.06 M)	1.01×10^{-3}	2.23×10^{-4}	5.65×10^{-6}	3.75×10^{-7}
50 (V(Ⅳ)=0.1 M)	5.34×10^{-4}	3.00×10^{-4}	2.11×10^{-6}	7.46×10^{-7}
30 (V(Ⅳ)=0.14 M)	3.32×10^{-4}	2.01×10^{-4}	8.65×10^{-7}	1.27×10^{-6}
10 (V(Ⅳ)=0.18 M)	2.35×10^{-4}	1.14×10^{-3}	5.24×10^{-7}	1.61×10^{-5}

Table 2. Diffusion coefficient and rate constants of V(Ⅱ)/V(Ⅲ) couple for different SOC

SOC/%	k_a/cm·s^{-1}	k_c/cm·s^{-1}	D_a/cm^2·s^{-1}	D_c/cm^2·s^{-1}
90 (V(Ⅲ)=0.04 M)	2.50×10^{-5}	3.82×10^{-4}	4.28×10^{-8}	9.86×10^{-6}
70 (V(Ⅲ)=0.12 M)	2.75×10^{-5}	1.94×10^{-4}	6.09×10^{-8}	1.01×10^{-6}
50 (V(Ⅲ)=0.2 M)	8.64×10^{-5}	2.53×10^{-4}	1.79×10^{-7}	6.53×10^{-7}
30 (V(Ⅲ)=0.28 M)	4.40×10^{-5}	9.52×10^{-5}	1.95×10^{-7}	1.73×10^{-7}
10 (V(Ⅲ)=0.36 M)	4.69×10^{-4}	1.16×10^{-4}	8.55×10^{-6}	2.51×10^{-7}

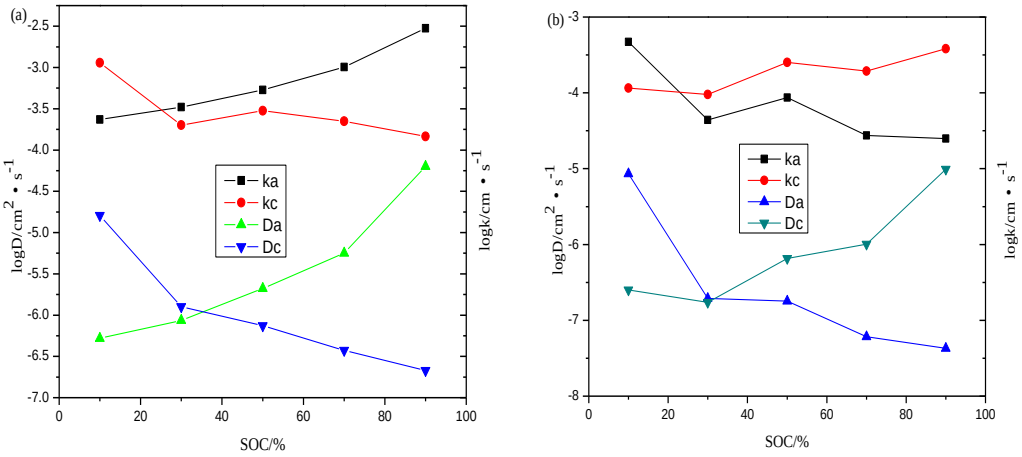

Figure 6. Diffusion coefficient and the rate constants for different SOC.(a) V(Ⅳ)/V(Ⅴ) couple, (b) V(Ⅱ)/V(Ⅲ) couple.

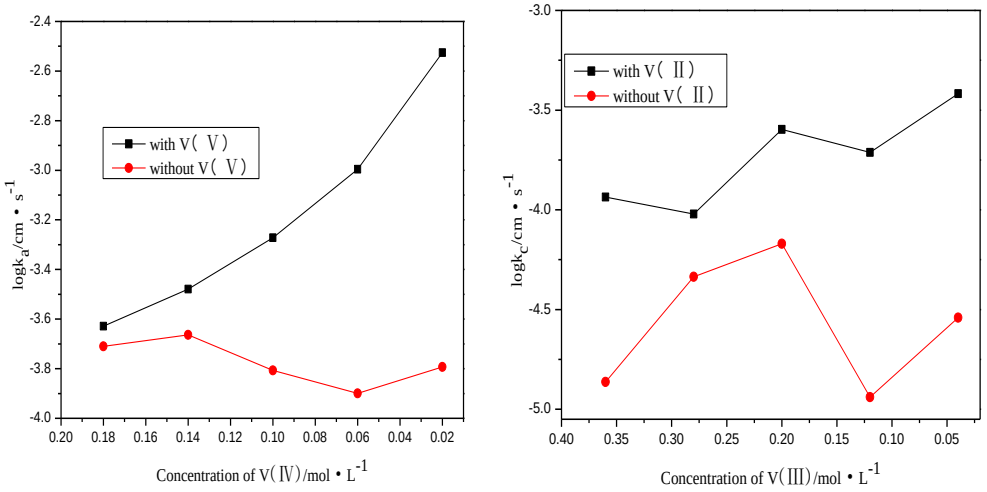

Figure 7. The rate constants for different concentration of vanadium ion. (a) V(Ⅳ)→V(Ⅴ) with and without V(Ⅴ), (b) V(Ⅲ)→V(Ⅱ) with and without V(Ⅱ)

The cyclic voltammetric study of V(Ⅳ)/V(Ⅴ) and V(Ⅱ)/V(Ⅲ) couples shows that at the ending of charge, electrode reaction is much faster and the potential goes up quickly, which may result in the corrosion of electrode and side reaction. Therefore, reasonable control the potential changing could avoid the reduction of capacitance and extend the cycle life of vanadium battery.

3.3. EIS characteristics for V(Ⅳ)/V(Ⅴ) and V(Ⅱ)/V(Ⅲ) couples

3.3.1. EIS measurements for V(Ⅳ)/V(Ⅴ) and V(Ⅱ)/V(Ⅲ) couples

Fig. 8 and 9 are EIS diagrams of V(Ⅳ)/V(Ⅴ) and V(Ⅱ)/V(Ⅲ) couples at a graphite electrode for different SOC which suggest that electrode process of V(Ⅳ)/V(Ⅴ) is quite similar to that of V(Ⅱ)/V(Ⅲ) couple.

The Nyquist plots are characterized with capacitive semicircles in the high frequency, and then in the low frequency the capacitive semicircles are combined to the straight line which is typical Warburg character, implying that both the electrochemical process and diffusion process played important roles in V(Ⅳ)/V(Ⅴ) and V(Ⅱ)/V(Ⅲ) couples [23]. Nyquist plots with a semicircles in the high frequency presents double-layer capacity. In this stage, the electron-transfer control electrode processes. The Warburg tail in the low frequency region shows that electrode processes are mass-transfer controlled. The Bode plots show relative little variations, indicating that the mechanisms of reaction for the two couples are in a relatively stable state with the values of |Z| around 17 $\Omega \cdot cm^2$ and 8 $\Omega \cdot cm^2$, respectively, with the rising of SOC.

Usually, the resistance between working electrode and auxiliary electrode can be estimated by the value of $|Z|_{f\to 0}$ in the modulus Bode plots. The higher value of $|Z|_{f\to 0}$ implies a lower reaction rate on the electrode. Fig. 11(b) shows that reaction rate of V(Ⅳ)/V(Ⅴ) couple is slower since the value of $|Z|_{f\to 0}$ of V(Ⅳ)/V(Ⅴ) couple is larger than that of V(Ⅱ)/V(Ⅲ) couple. Similarly, the values of charge transfer resistance (Rt) for V(Ⅱ)/V(Ⅲ) couple is smaller than that of V(Ⅳ)/V(Ⅴ) couple in Fig. 11(a) validates that reaction rate of V(Ⅳ)/V(Ⅴ) couple is slower, which is contradictory with the results from cyclic voltammetry. The cyclic voltammograms results reveal that the reaction rate of V(Ⅳ)/V(Ⅴ) couple is quite quicker than that of V(Ⅱ)/V(Ⅲ) couple at graphite electrode. The reason might cause by side reaction of hydrogen in cyclic voltammograms, characteristic of gas evolving is the formation of gas bubbles. The presence of the bubbles [2] reduces the liquid-phase volume in the electrodes, leading to a restricted flow of the electrolyte, a reduced active surface area for V(Ⅱ)/V(Ⅲ) reaction, which lead to the contradiction results between cyclic voltammograms and EIS.

The flattened semicircle of positive electrode on account of dispersion effect is caused by asymmetrical property of interface between electrode and electrolyte. Plots in Fig. 8 and Fig. 9 can be described using the equivalent circuit shown in Fig. 10. Values of Rt and $|Z|_{f\to 0}$ based on equivalent circuit of V(Ⅳ)/V(Ⅴ) and V(Ⅱ)/V(Ⅲ) couples for different SOC are shown in Fig. 11.

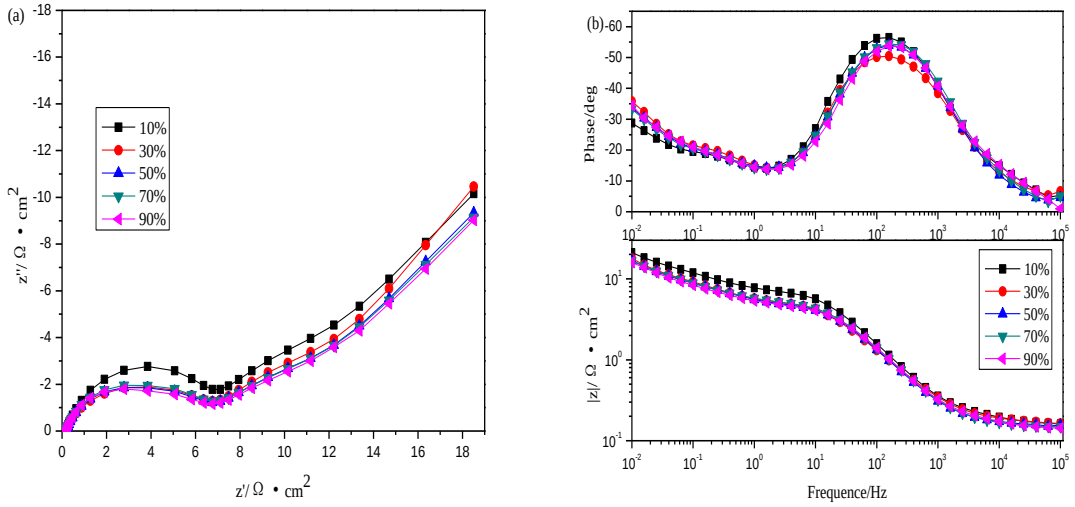

Figure 8. EIS plots of V(Ⅳ)/V(Ⅴ) couple at polarization potential of 0.8 V vs. SCE for different SOC: (a)Nyquist plots; (b)Bode plots

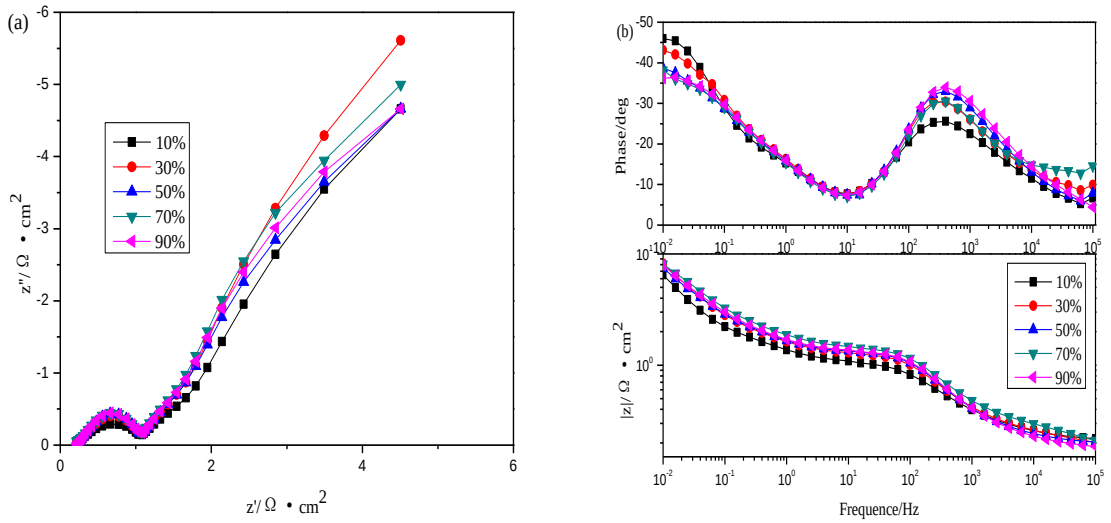

Figure 9. EIS plots of V(Ⅱ)/V(Ⅲ) couple at polarization potential of -0.5 V vs. SCE for different SOC: (a)Nyquist plots; (b)Bode plots

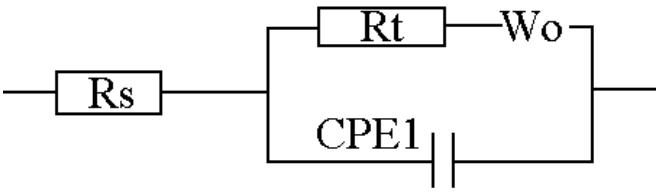

Figure 10. Equivalent circuits proposed for fitting of EIS plots in Fig. 8 and 9, Rs is the electrolyte resistance, Rt is the charge transfer resistance, corresponding to resistance of electrode reaction, CPE1 is the constant-phase element used to replace Cp, the double layer capacitance, Wo is corresponding to the Warburg impedance, account for diffusion ability of vanadium ions.

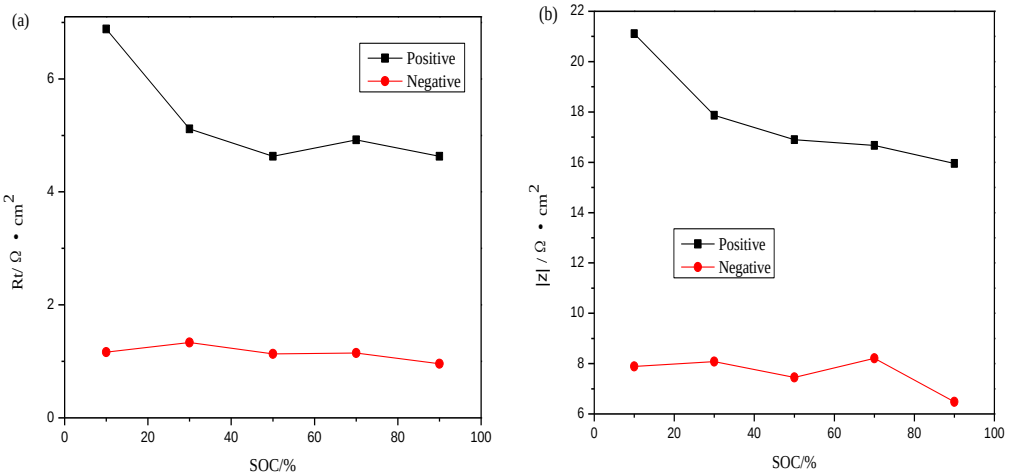

Figure 11. The evolution of circuit parameters for V(Ⅳ)/V(Ⅴ) and V(Ⅱ)/V(Ⅲ) couples at graphite electrode for different SOC

3.3.2. Electrochemical reaction mechanism for V(Ⅳ)/V(Ⅴ) and V(Ⅱ)/V(Ⅲ) couples

Normally, the overall reactions of V(Ⅳ)/V(Ⅴ) and V(Ⅱ)/V(Ⅲ) couples occurring at both electrodes are typically written as shown below [24].

$$VO_2^+ + 2H^+ + e^- \rightarrow VO^{2+} + H_2O \quad (3)$$

$$V^{2+} \rightarrow V^{3+} + e^- \quad (4)$$

The values of $|Z|_{f\rightarrow 0}$ and Rt in Fig. 11 for the two reaction indicate that the kinetics of V(Ⅳ)/V(Ⅴ) couple are slower than that of V(Ⅱ)/V(Ⅲ) couple (see also [24]). These facts might suggest that V(Ⅳ)/V(Ⅴ) redox process (Eq.(3)) is not simple and the electron transfer is followed by a certain chemical step, which has been found in previous work [18-19]. The equivalent circuit in Fig. 10 reflected electrode reaction processes of V(Ⅳ)/V(Ⅴ) and V(Ⅱ)/V(Ⅲ) couples at a graphite electrode. Rt and Wo associate to electrochemical polarization and concentration polarization for V(Ⅳ)/V(Ⅴ) and V(Ⅱ)/V(Ⅲ) couples, respectively. Cp replacing by CPE1 corresponds to dispersion effect due to roughness of electrode surface. The decreased values of $|Z|_{f\rightarrow 0}$ and Rt responds to the growth of reaction rate for V(Ⅳ)/V(Ⅴ) couple with rising of SOC which is consistent with the results in Fig. 6(a). Values of $|Z|_{f\rightarrow 0}$ and Rt for V(Ⅱ)/V(Ⅲ) couple are changeless mean that reaction rate of the couple at a graphite electrode is quite not dependent on SOC. The rate constants increase gradually for different SOC in Fig. 7 are likely to be caused by evolution of hydrogen, which is not accounted for in the present paper but are explored in the forthcoming study.

4. CONCLUSIONS

The electrons transfer of V(Ⅳ)/V(Ⅴ) and V(Ⅱ)/V(Ⅲ) couples had been found to be electrochemically irreversible at the graphite electrode by cyclic voltammograms. The variation of rate constant (k) and diffusion coefficient (D) was consistency with the state of charge (SOC), namely, the values of D_a, k_a of V(Ⅳ)/V(Ⅴ) couple and D_c, k_c of V(Ⅱ)/V(Ⅲ) couple were improved with increasing of SOC. The potential went up quickly at the end of charge.

The electrode processes of V(Ⅳ)/V(Ⅴ) and V(Ⅱ)/V(Ⅲ) couples were controlled by both electron-transfer and mass-transfer by EIS. In vanadium redox flow battery, the electron transfer of V(Ⅱ)/V(Ⅲ) couple was much faster than that of V(Ⅳ)/V(Ⅴ) couple at graphite electrode. There might be a certain chemical step concerned with the process of electron transfer for V(Ⅳ)/V(Ⅴ) couple. Necessary future efforts concerned the control of hydrogen evolution in cathode of battery and increased the current density of V(Ⅱ)/V(Ⅲ) couple to ensure charge and discharge balances of positive and negative.

ACKNOWLEDGEMENTS

Financial support from Shenyang Agricultural University Postdoctoral Fund is gratefully acknowledged.

References

1. H. Al-Fetlawi, A.A. Shah, F.C. Walsh, *Electrochim. Acta* 55 (2009) 78.
2. H. Al-Fetlawi, A.A. Shah, F.C. Walsh, *Electrochim. Acta* 55 (2010) 3192.
3. A.A. Shah, H. Al-Fetlawi, F.C. Walsh, *Electrochim. Acta* 55 (2010) 1125.
4. A. Hazza, D. Pletcher, R. Wills, *J.Powe Sources* 149 (2005) 103.
5. D. Pletcher, H. Zhou, G. Kear, C.T.J. Low, F.C. Walsh, R. Wills, *J. Power Sources* 180 (2008) 62.
6. D. Pletcher, H. Zhou, G. Kear, C.T.J. Low, F.C. Walsh, R. Wills, *J. Power Sources* 180(2008) 630.
7. C. Ponce de León, A. Frías-Ferrer, J. González-García, D.A. Szánto , F.C. Walsh, *J. Power Sources* 160 (2006) 716.
8. Ch. Fabjan, J. Garche, B. Harrer, L. Jo¨rissen, C. Kolbeck, F. Philippi, G. Tomazic, F. Wagner, *Electrochim. Acta* 47 (2001) 825.
9. L.H. Thaller, US Patent 3,996,064, US, 1976.
10. Y.H. Wen, J. Cheng, H.M. Zhang, Y.S.Yang, *Batttery Bimonthly* 38 (2008) 247.
11. M.H. Chakrabarti, R.A.W. Dryfe, E.P.L. Roberts, *Electrochim. Acta* 52 (2007) 2189.
12. M. Rychcik, M. Skyllas-Kazacos, *J. Power Sources* 22 (1988) 59.
13. E.Sum, M.Rychcik, M.Skyllas-Kazacos, *J. Power Sources* 16 (1985) 85.
14. E.Sum, M.Skyllas-Kazacos. *J. Power Sources* 15 (1985) 179.
15. S.Zhong, M.Skyllas-Kazacos, *J. Power Sources* 39 (1992) 17.
16. S.Iwasa, Y.Wei, B.Fang, T. Arai, M.Kumagai, *Battery bimonthly* 33(6) (2003) 339.
17. G. Oriji, Y. Katayama, T. Miura, *Electrochim. Acta* 49 (2004) 3091.
18. G. Oriji, Y. Katayama, T. Miura, *J. Power Sources* 139 (2005) 321.
19. M.Gattrell, J.Park, B.MacDougall, J. Apte, S.McCarthy, C.W. Wu, *J. Electrochem. Soc*. 151 (2004) A123.
20. F. Y. Chen, J. G. Liu, H. Chen, C. W. Yan, *Int. J. Electrochem. Sci.* 7 (2012) 3750.
21. H. J. Liu, Q. Xu, C. W. Yan, Y. L. Qiao, E*lectrochim. Acta* 56 (2011) 8783.
22. A.J.Bard, L.R.Faulkner(eds.), Electrochemical Methods and Applications, Wiley, New York, 1980, 213.
23. H.L. Hu, N. Li, *Electrochemical measurement*, Beijing, 2007, 224.
24. M. Gattrell, J. Qian, C. Stewart, P. Graham, B.MacDougall, *Electrochim. Acta* 51 (2005) 395.